

# Experimental Demonstration of Photon Efficient Coherent Temporal Combining for Data Rate Scaling

D. J. Geisler, T. M. Yarnall, M. L. Stevens, C. M. Schieler, B. S. Robinson, and S. A. Hamilton  
MIT Lincoln Laboratory, 244 Wood St., Lexington, MA 02421

## ABSTRACT

The next generation free-space optical (FSO) communications infrastructure will need to support a wide range of links from space-based terminals at LEO, GEO, and deep space to the ground. Efficiently enabling such a diverse mission set requires a common ground station architecture capable of providing excellent sensitivity (*i.e.*, few photons-per-bit) while supporting a wide range of data rates. One method for achieving excellent sensitivity performance is to use integrated digital coherent receivers. Additionally, coherent receivers provide full-field information, which enables efficient temporal coherent combining of block repeated signals. This method allows system designers to trade excess link margin for increased data rate without requiring hardware modifications. We present experimental results that show a 45-dB scaling in data rate over a 41-dB range of input powers by block-repeating and combining a PRBS sequence up to 36,017 times.

**Keywords:** digital signal processing, optical receivers, phase shift keying, coherent combining

## 1. INTRODUCTION

Future space-based free-space optical (FSO) communication systems will need to support a wide diversity of missions<sup>1-4</sup>. For example, terminals located in Earth orbit could support data links with user rates in the 10's to 100's of Gb/s<sup>5</sup>. Other links operating at greater distances may be called upon to provide significantly lower rates in order to contend with the concomitant increase in link loss. Designing a specialized terminal pair optimized for each use case is a potential path to supporting this variety of missions; however, it would involve costly custom hardware development for each scenario. As an alternative approach, a modem design that can operate at high rate when losses are small and then fall back to lower rates as losses increase enables a single hardware design that can support a wide range of mission requirements. In the context of this paper this trade-off is referred to as 'rate scaling'.

Wide dynamic-range data-rate scaling (>20 dB range of data rates) is difficult to achieve with a single hardware architecture while maintaining excellent sensitivity and minimizing the size, weight, and power (SWaP) on the space platform. Existing approaches to rate scaling with sensitive performance generally cover a <20 dB range of data rates and use custom optical modems for each specific mission scenario (*e.g.*, references<sup>6-11</sup>). One approach uses pulse-position modulation (PPM), which has been demonstrated experimentally to achieve sensitivities within 0.23-dB of PPM theory<sup>6</sup>. Experimental demonstrations using PPM with variable slot rates and variable number of slots achieved a 12-dB range of data rates from 38 - 622 Mb/s with sensitivity performance less than 1.1-dB from PPM theory<sup>6,7</sup>. Other approaches use burst-rate differential phase-shifted keying (DPSK) to achieve rate scaling by varying the signal duty cycle over a 16-dB range of data rates from 36 Mb/s - 1.44 Gb/s<sup>8,9</sup>. Another experimental demonstration using burst-rate DSPK achieved a 30-dB range of data rates from 2.4-Mb/s to 2.5-Gb/s while maintaining sensitivity performance within 1.0-dB of DPSK theory<sup>10</sup>. The lower bound on data rate scaling for pre-amplified PPM and burst-rate DPSK systems is governed by nonlinearities induced from amplification of low duty-cycle signals<sup>10</sup>. M-ary frequency shift keying (FSK) has also been demonstrated as a technique capable of achieving sensitivities within 1.5 dB of FSK theory while enabling rate scaling from Mb/s to Gb/s using a custom receiver architecture<sup>11</sup>.

Another method for rate scaling involves repeating and digitally combining blocks of symbols in an effort to reduce the effective data rate while maintaining the same symbol rate, thus not requiring any changes to the hardware architecture. Experimental demonstrations have already shown that rate scaling using incoherent combining with pre-amplified

---

Distribution A: Public Release. This work was sponsored by the Assistant Secretary of Defense for Research and Engineering under Air Force Contract #FA8721-05-C-0002. Opinions, interpretations, conclusions, and recommendations are those of the authors and are not necessarily endorsed by the United States Government.

receivers can only achieve a 1.5-dB signal-to-noise (SNR) improvement for every doubling of the number of block repeats<sup>9</sup>. This places a practical lower bound on the achievable data rates since a reduction of  $N$  in data rate requires  $N^2$  block repeats. Systems using incoherent combining with photon counting receivers can achieve a 3-dB SNR improvement, but are limited to maximum data rates of  $\sim 1 \text{ Gb/s}^{2,7}$ . Alternatively, coherent combining with pre-amplified receivers can be used, which provides a 3-dB SNR improvement for each doubling of the number of block repeats. Recent experimental demonstrations have shown the practical viability of the 3-dB SNR improvement by coherently combining a common block of data received by parallel receivers (*i.e.*, spatial coherent combining)<sup>12</sup>.

Recent advances by the fiber telecom industry towards the development of high-rate high-sensitivity digital coherent receivers have enabled the capability for practical coherent combining. Using digital coherent receivers to detect the full-field (*i.e.*, in-phase and quadrature-phase components) of the optical waveform, experimental demonstrations have achieved sensitivities of 2-3 dB photons-per-bit (PPB) at multi-gigabit data rates<sup>13,14</sup>. Using block repeating and coherent combining does not impose a fundamental architecture limitation to the lowest achievable data rate. However, there are practical limits that will ultimately be reached due to implementation effects, such as laser linewidth, clock instability, other sources of phase noise, or channel effects, such as atmospheric coherence time.

In this paper, experimental results show the ability to achieve 45-dB rate scaling using block repeating and coherent combining. This form of temporal coherent combining enables a nearly one-to-one trade of excess margin for data rate while maintaining a constant system symbol rate. Specifically, 36,017 repetitions of an 11.52-GBd BPSK waveform enable reducing the data rate to 320-kb/s with minimal implementation penalty and without requiring any changes to the transmitter or receiver hardware architecture.

This paper is organized as follows. Section 2 discusses the advantages and limits of data rate scaling using block repeating and coherent combining. Section 3 and Section 4 describe the experimental arrangement and results, respectively, for the presented block repeating and coherent combining experiment. Section 5 summarizes the paper.

## 2. DATA RATE SCALING

Rate scaling can be implemented by changing various system parameters, such as symbol rate, modulation format, or by repeating blocks of data symbols<sup>9,15</sup>. A major challenge for rate scaling is to maintain excellent receiver sensitivity while operating over as wide a dynamic range of data rates as possible. Changing the symbol rate can provide the most granularity for choosing a desired data rate. However, adjusting the symbol rate can require changes to the transmitter and receiver hardware, especially in FSO systems that use pulse carving. Changing the transmitter hardware for each change in data rate is not a feasible option for a space-borne platform. Other transmitter solutions involve the use of multi-level digital-to-analog convertors (DACs) that can be expensive to implement and negatively influence SWaP. Changing the modulation format can also affect the achievable data rate, but it becomes complicated for a transmitter and receiver architecture to support multiple modulation formats while maintaining excellent sensitivity.

Block repeating is a technique for rate scaling that does not require changes to the transmitter or receiver high-speed electronics or optics hardware. In block repeating, each block of a specified number of data symbols,  $S$ , is repeated  $N$  times by the transmitter. The receiver then combines the repeated blocks in digital signal processing (DSP). The repeated block can be combined incoherently by power combining for a  $\sqrt{N}$  improvement in SNR, or coherently which results in an  $N$  improvement in SNR since the phases of the signals being combined can be phase aligned. Coherent combining is more efficient, but requires a phase sensitive receiver, such as a digital coherent receiver. Recent results have shown pre-amplified digital coherent receivers to achieve excellent sensitivity ( $\sim 2$  dB from theory) over  $\sim 20$  dB dynamic range<sup>13,14</sup>. By combining digital coherent receivers with block repeating it is possible to further extend the achievable data rate dynamic range. Figure 1 shows how increasing the number of block repeats results in a decrease in data rate and an increase in the link margin, which enables extending the achievable transmission distance or relaxing other system parameters.

Block repeating and coherent combining requires that the carrier phase be known and tracked for the total time duration of each set of block repeats to be coherently combined. The data rate can be lowered by coherently combining block repeats as long as the relative phase between each block can be determined. To help further simplify the transmitter and receiver in a block repeating with coherent combining system, it could be advantageous to set the block length equal to a forward error correction (FEC) codeword length as opposed to an arbitrary length. The temporal coherence time is governed by the smaller of two major components: laser coherence time and atmospheric coherence time. The laser coherence time is roughly equal to the inverse of its linewidth. For example, the coherence time of a 10-kHz linewidth

laser is  $\sim 100 \mu\text{s}$ . On the other hand, the atmospheric coherence time will be a function of the particular atmospheric conditions and is on the order of  $\sim 1\text{-}10 \text{ ms}$ <sup>16</sup>. Readily available commercial off-the-shelf lasers that have linewidths on the order of 10 kHz are likely to be the limiting factor for the temporal coherence time in most atmospheric conditions.

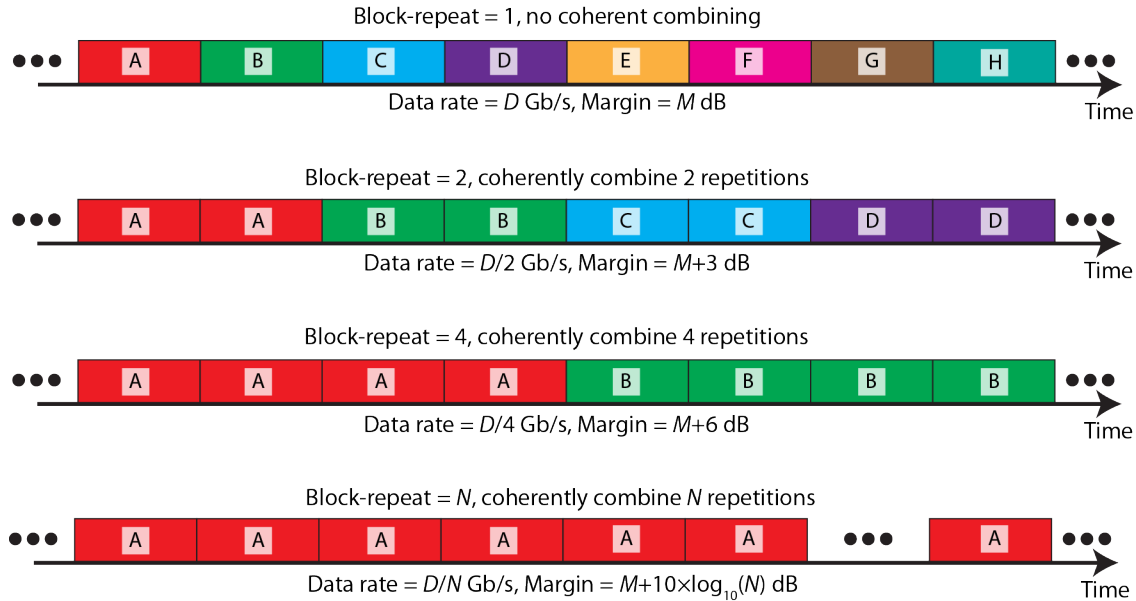


Figure 1. Block repeating and coherent combining concept. Letters A-H represent unique blocks of bits.

### 3. BLOCK REPEATING AND COHERENT COMBINING EXPERIMENTAL ARRANGEMENT

The concept of block repeating is dependent on having a known carrier phase in the received signal over a specified time interval. The relative phase offset of each block to be combined can be estimated by calculating the mean of the dot products of samples in each block with respect to one block which is defined as the reference. The relative phase offset for each block is then removed allowing the corresponding data samples in all the blocks to be added to achieve high SNR and then demodulated using carrier phase estimation. As described in Section 2, the block time over which the temporal phase can be assumed constant is limited by the laser coherence length (signal or LO) or the atmospheric coherence time, whichever is shorter. Figure 2 shows the experimental setup used to demonstrate block repeating over a wide range of data rates. This particular experimental arrangement was configured to minimize phase variations due to both laser linewidth and atmospheric coherence time to show that block repeating can be effective over a reasonably long time duration. Here, we observed a 6.4-ms time duration for each data acquisition, which was only limited by the real-time scope memory depth.

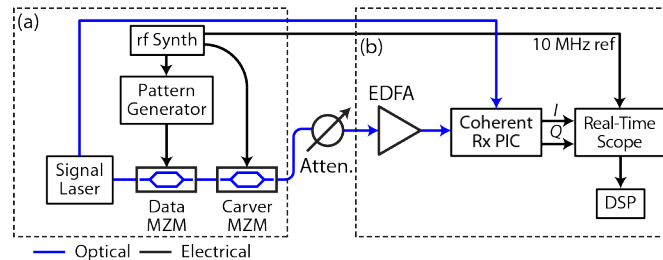


Figure 2. Experimental arrangement showing (a) the transmitter and (b) the pre-amplified coherent receiver. MZM: Mach-Zehnder modulator. DSP: digital signal processing.

The transmitter and receiver were in an autodyne configuration, which means that a tap from the signal laser prior to modulation was used as the local oscillator in the receiver. The result is that the effects of laser linewidth were effectively negated since frequency and phase variations of the signal laser would be common along the signal and LO

paths as long as the path length difference is less than the phase coherence time of the laser. In a real system, laser linewidth can be removed as a significant source of error by using low linewidth ( $<1$  kHz) signal and LO lasers. Here, using a fiber-based setup enabled ignoring the effect of atmospheric coherence time. In FSO systems, the atmospheric coherence time is dependent on the specific atmospheric conditions, but is on the order of 1-10 ms.

Figure 2(a) shows the transmitter used to generate the 11.52-GBd binary phase-shifted keying (BPSK) waveform. The signal laser, a fiber laser with a 10-kHz linewidth, was data modulated and pulse carved by two serially concatenated Mach-Zehnder modulators (MZM). The use of two independent modulators avoided the need for high-speed multi-level digital-to-analog converter (DAC) signals since the data and pulse carver MZMs could be driven by a binary signal and a clock signal, respectively. In particular, the use of a pulse carving modulator created pulses with a 50-% return-to-zero (RZ-50) pulse shape that enabled matched filtering at the receiver and also provided a strong clock tone to aid in the clock recovery process. The drive signal for the data MZM was a  $2^{11}$ -1 length pseudo-random bit sequence (PRBS).

After the transmitter, the signal passed through an attenuator and underwent pre-amplified coherent detection (Figure 2(b)). Specifically, the pre-amplified coherent detection process consisted of two stages of amplification and filtering followed by a  $90^\circ$ -optical hybrid and two pairs of balanced photodiodes. Next, a real-time scope acquired the in-phase ( $I$ ) and quadrature phase ( $Q$ ) components of the received optical waveform. Note that the 10-MHz reference signal between the RF synthesizer and the real-time scope were synchronized to minimize timing errors between the transmitter and receiver. Each 6.4-ms real-time scope trace yielded 36,017 complete repetitions of the PRBS. Digital signal processing (DSP) enabled implementing the block repeats and the other necessary operations for symbol demodulation and bit-error rate (BER) analysis.

Specifically, the DSP algorithm implemented blind combining, in which the block repeats were coherently combined under the assumption that there is an insignificant amount of phase noise over the entire 6.4-ms acquisition. The DSP algorithm first interpolates the acquired samples to be an integer number of samples per symbol. Next, the desired number of repetitions of the PRBS were isolated and coherently added. Next, the DSP algorithm adjusted the signal phase so that the two BPSK constellation points were aligned to 0 and  $\pi$  phase, applied an RZ-50 matched filter, determined the start time of the PRBS pattern, and measured the BER.

#### 4. BLOCK REPEATING AND COHERENT COMBINING EXPERIMENTAL RESULTS

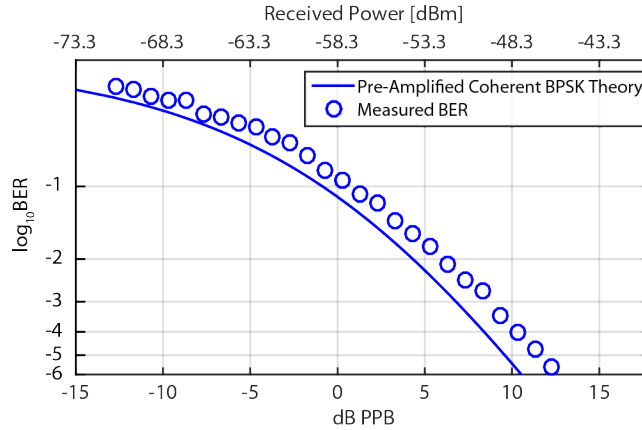


Figure 3. Measured results of BPSK BER performance without block-repeating temporal coherent combining.

Figure 3 shows the BER result without block-repeating and temporal coherent combining for 1,000 repetitions (*i.e.*, 2,047,000 bits at each power level) of the 11.52-GBd BPSK PRBS sequence taken at various power levels. Note that the digital coherent receiver achieved close to theoretical performance ( $\sim 2$  dB penalty) over a  $>20$  dB range of input powers. Here, the evaluation of 2,047,000 bits at each power level enabled BER values as low as  $2 \times 10^{-5}$  to be accurately determined.

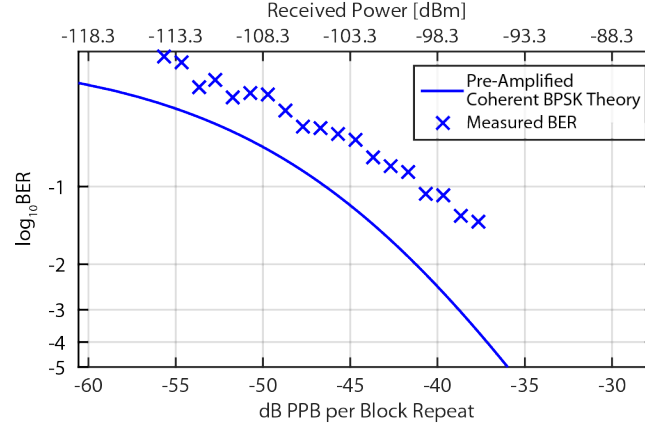


Figure 4. Measured results of BPSK BER performance with block-repeat temporal coherent combining of 36,017 waveform repetitions.

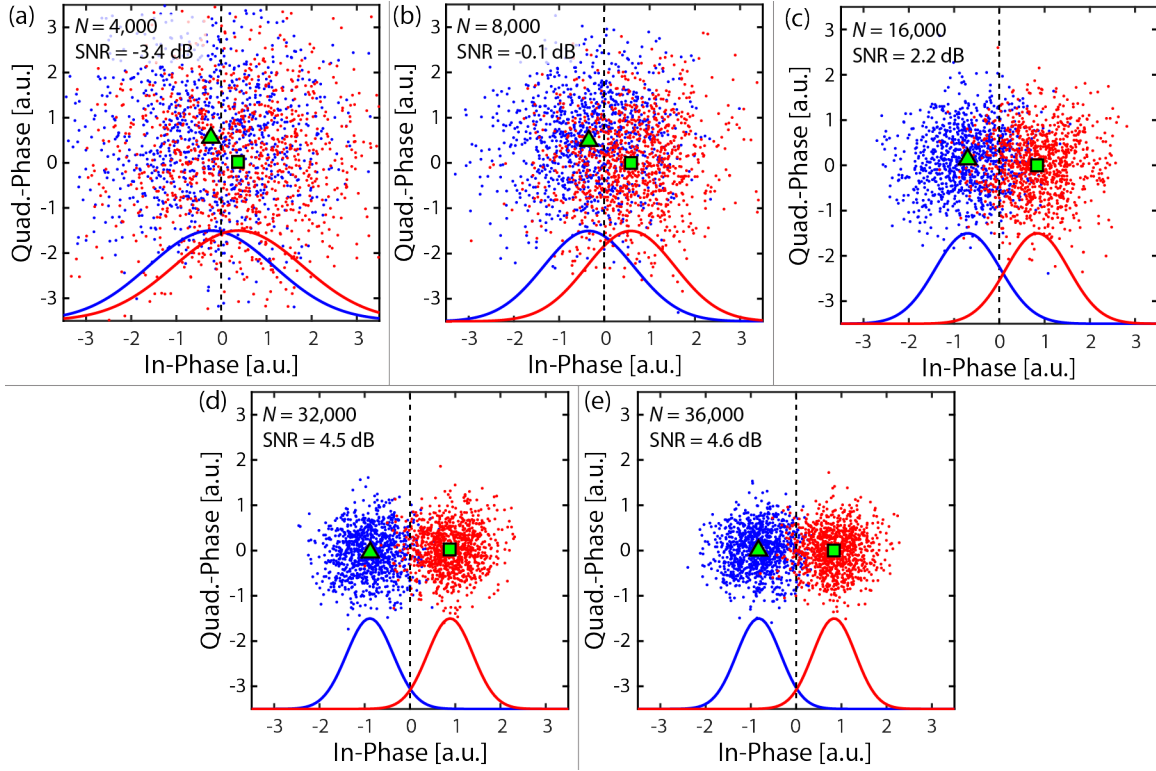


Figure 5. Constellation diagram for -96 dBm signal with  $2^{11}$ -1 points after block repeating and combining the waveform various number of block repeats ( $N$ ). The blue dots and red dots represent the measured symbol field for the 1's and 0's values, respectively. The blue and red curves represent the marginal probability density function for the 1's and 0's values, respectively. The green triangle and square represent the centroid for the 1's and 0's values, respectively.

Figure 4 shows the BER result for the  $2^{11}$ -1 PRBS pattern after temporally coherently combining 36,017 repetitions. The number of waveform repetitions yields a 45.6 dB reduction in data rate from 11.52 Gb/s to 319.8 kb/s after block repeating and temporal coherent combining. The measured results trend with the BPSK theory curve at  $\sim 5$  dB from theory, which is an additional  $\sim 3$  dB penalty from block-repeat theory. The additional penalty is likely due to temporal phase changes in the laser due to acoustic, thermal, or vibrational drift in the laboratory setup over the 6.4-ms long

acquisitions that led to imperfect blind coherent combining. There could also be residual timing offsets between the transmitter and receiver sampling clocks that led to coherent combining errors as the number of block repeats increased.

Observing the effect of block repeating as a function of the number of repetitions being coherent combined provides an indication of the efficacy of the block repeating over the 6.4-ms duration data sets. In particular, Figure 5 shows constellation diagrams for the -96 dBm signal after temporal coherent combining of 4,000, 8,000, 16,000, 32,000, and 36,000 block repeats. Note that after 4,000 block repeats (Figure 5(a)), the two constellation points are still mostly overlapping. The marginal probability distribution of the 1's and 0's symbols have nearly zero mean and have large standard deviations with respect to the window size. As the number of block repeats increases, however, the mean of the marginal probability distributions increases and the standard deviations decrease. The slight rotation of the constellation points is indicative of residual phase offset relative to the optimal phase at 36,000 block repeats caused by either thermal or vibrational effects.

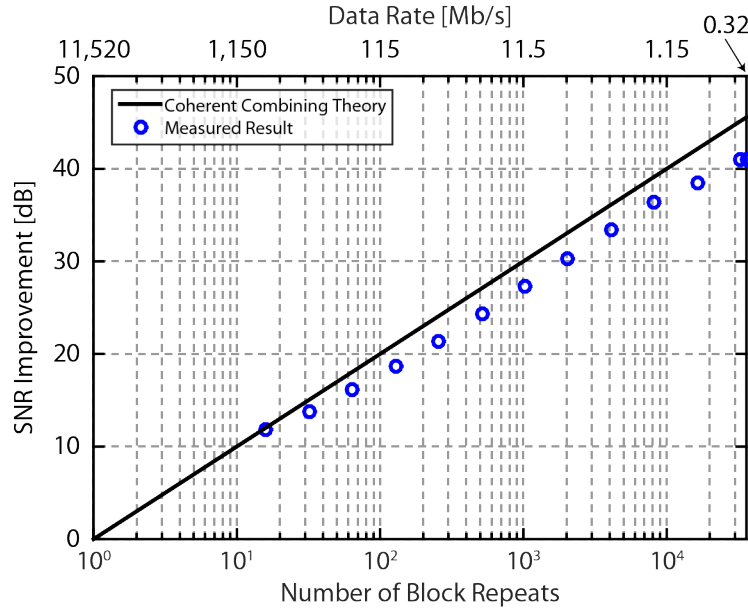


Figure 6. SNR improvement vs. number of block repeats for the -96 dBm signal.

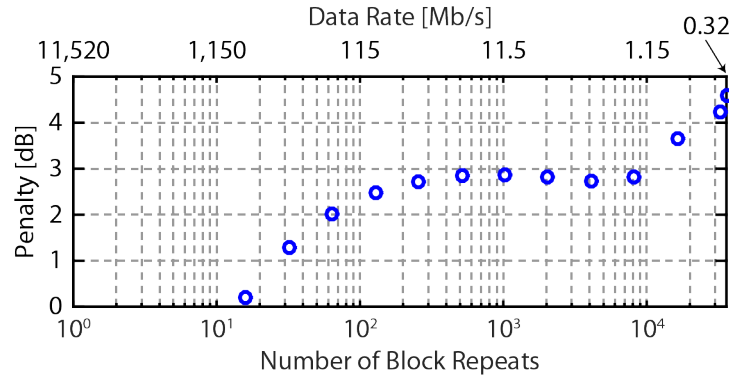


Figure 7. Coherent combining penalty vs. number of block repeats for the -96 dBm signal.

Figure 6 shows the SNR improvement as a function of the number of block repeats for the -96 dBm signal. It can be seen that the improvement to SNR tapers off for large number of block repeats, which is likely a result of the finite coherence time of the experimental setup. Figure 7 shows the penalty from optimal combining achieved as a function of the number of block repeats. Starting in the 10's to 100's of block repeats the penalty from coherent combining increases from a negligible amount to approximately 3-dB, possibly as a result of acoustic, timing, or other noise sources that become significant for coherence times  $>2 \mu\text{s}$ . Additional penalty is introduced after combining more than 10,000 block repeats,

which corresponds to phase coherence times  $>2$  ms that is potentially thermal in origin. Improved performance could likely be obtained by tracking the slowly varying phase over the 6.4-ms data acquisitions and by implementing a clock recovery algorithm in the DSP to compensate for residual timing offsets between the transmitter and receiver sampling clocks.

## 5. CONCLUSION

Developing an optical transmission system capable of data rate scaling over several orders of magnitude of data rates is a challenge with a single hardware architecture while maintaining excellent sensitivity. Block repeating and coherent combining is one such technique that can scale over four orders of magnitude of data rates by repeating a block of symbols a specified number of times and coherently combining the measured result in DSP. In this paper, we presented experimental results of block repeating and coherent combining to achieve a 45-dB range of data rates. Using this technique enabled the demonstration of data rate scaling from 11.52 Gb/s to 320 kb/s.

## REFERENCES

- [1] D. M. Cornwell, "NASA's optical communications program for 2015 and beyond," in *Proc. SPIE 9354, Free-Space Laser Communication and Atmospheric Propagation XXVII*, 93540E, 2015.
- [2] S. A. Townes, B. L. Edwards, A. Biswas, D. R. Bold, R. S. Bondurant, D. M. Boroson, *et al.*, "The Mars laser communication demonstration," in *Proc. of IEEE Aerospace Conference*, 2004, pp. 1180-1195 Vol.2.
- [3] V. W. S. Chan, "Optical Satellite Networks," *J. Lightw. Technol.*, vol. 21, pp. 2811-2827, 2003.
- [4] M. Toyoshima, "Trends in satellite communications and the role of optical free-space communications," *J. Opt. Netw.*, vol. 4, pp. 300-311, 2005.
- [5] D. M. Boroson, B. S. Robinson, C. M. Schieler, F. I. Khatri, S. Constantine, B. Reid, M., *et al.*, "A New Optical Communication Architecture for Delivering Extremely Large Volumes of Data from Space to Ground," in *Proc. of AIAA SPACE 2015 Conference and Exposition*, 2015, doi:10.2514/6.2015-4658.
- [6] M. L. Stevens and D. M. Boroson, "A simple delay-line 4-PPM demodulator with near-optimum performance," *Opt. Express*, vol. 20, pp. 5270-5280, 2012.
- [7] M. M. Willis, B. S. Robinson, M. L. Stevens, B. R. Romkey, J. A. Matthews, J. A. Greco, *et al.*, "Downlink Synchronization for the Lunar Laser Communications Demonstration," in *Proc. 2011 International Conference on Space Optical Systems and Applications (ICSOS)*, 2011, pp. 83-87.
- [8] M. A. Kraniak, E. Luhanskiy, S. X. Li, S. A. Merritt, A. W. Yu, R. Butler, *et al.*, "A dual format communication modem development for the Laser Communications Relay Demonstration (LCRD) program," in *Proc. of SPIE 8610, Free-Space Laser Communication and Atmospheric Propagation XXV*, 86100K, 2013.
- [9] N. W. Spellmeyer, C. A. Browne, D. O. Caplan, J. J. Carney, M. L. Chavez, A. S. Fletcher, *et al.*, "A multi-rate DPSK modem for free-space laser communications," in *Proc. SPIE 8971, Free-Space Laser Communication and Atmospheric Propagation XXVI*, 89710J, 2014, 10.1117/12.2057568.
- [10] D. O. Caplan, H. G. Rao, J. P. Wang, D. M. Boroson, J. J. Carney, A. S. Fletcher, *et al.*, "Ultra-wide-range Multi-rate DPSK Laser Communications," in *Proc. of Conference on Lasers and Electro-Optics (CLEO)*, 2010, paper CPDA8.
- [11] D. O. Caplan, J. J. Carney, and S. Constantine, "Parallel Direct Modulation Laser Transmitters for High-speed High-sensitivity Laser Communications," in *Proc. of Conference on Lasers and Electro-Optics (CLEO)*, 2011, paper PDPB12.
- [12] T. M. Yarnall, D. J. Geisler, M. L. Stevens, C. M. Schieler, B. S. Robinson, and S. A. Hamilton, "Multi-Aperture Digital Coherent Combining for Next-Generation Optical Communication Receivers," in *Proc. 2015 International Conference on Space Optical Systems and Applications (ICSOS)*, 1570211585, 2015.
- [13] D. J. Geisler, V. Chandar, T. M. Yarnall, M. L. Stevens, and S. A. Hamilton, "Multi-gigabit Coherent Communications Using Low-Rate FEC to Approach the Shannon Capacity Limit," in *Conference on Lasers and Electro-Optics (CLEO)*, San Jose, CA, 2015, paper SW1M.2.
- [14] D. J. Geisler, T. M. Yarnall, W. E. Keicher, M. L. Stevens, A. S. Fletcher, R. R. Parenti, *et al.*, "Demonstration of 2.1 Photon-Per-Bit Sensitivity for BPSK at 9.94-Gb/s with Rate-1/2 FEC," in *Proceedings of Optical Fiber Communications Conference (OFC)*, Anaheim, CA, 2013, paper OM2C.6.

- [15]D. O. Caplan and J. J. Carney, "Power-efficient Noise-insensitive Optical Modulation for High-sensitivity Laser Communications," in *Conference on Lasers and Electro-Optics (CLEO)*, 2014, paper SM4J.6.
- [16]J. Davis and W. J. Tango, "Measurement of the Atmospheric Coherence Time," *Publications of the Astronomical Society of the Pacific*, vol. 108, pp. 456-458, 1996.